Effect of H insertion on the magnetic, electronic, and structural properties of CeCoSi

Bernard Chevalier, Samir F. Matar

Effect of H insertion on the magnetic, electronic, and structural properties of CeCoSi

B. Chevalier and S. F. Matar*
Institut de Chimie de la Matière Condensée de Bordeaux (ICMCB) -CNRS [UPR 9048], Université Bordeaux 1, 87 Avenue du Dr. Albert Schweitzer, F-33608 Pessac Cedex, France
(Received 9 April 2004; published 9 November 2004)

Contrary to other cerium equiatomic intermetallic systems (Ce*TX* with T=transition metal, $X=p$ metal) which become magnetically ordered upon hydrogen insertion, magnetic measurements characterize an antiferromagnet for CeCoSi and a spin fluctuation system for its hydride CeCoSiH. The presented results of electrical and magnetic properties of the silicide CeCoSi demonstrate the existence of an antiferromagnetic transition at $T_N=8.8(2)$ K. For the purpose of further assessing the experimental findings, the electronic and magnetic sructures of CeCoSi and CeCoSiH are self-consistently calculated within the local spin density functional LSDF theory. The analysis of the electronic structures and of the chemical bonding properties lead to suggest that the chemical effect of hydrogen prevails over the cell expansion effect which would enhance the magnetization otherwise. Spin orbit coupling effects on cerium are examined. A potential antiferromagnetic structure with a propagation along the c axis is proposed for CeCoSi ground state.

DOI: 10.1103/PhysRevB.70.174408 PACS number(s): 75.50.Ee, 75.30.Cr, 71.20.−b, 71.70.Ej

I. INTRODUCTION AND OBJECTIVES

Intermetallic systems based on cerium $Ce_XT_YX_Z$ (T =transition metal and $X=p$ metal) are known to exhibit a wide variety of electronic properties such as heavy fermions, valence fluctuation, magnetic ordering, etc.[1–3] The underlying physics of these properties is relevant to the degree of hybridization between the (f) states and the conduction electrons (c). The interaction at each lattice site, between conduction electrons and localized $4f$ electrons is described by the Kondo model whereby conduction electrons are spin polarized due to their exchange interaction with the localized $4f$ electrons. This spin polarization propagates from one lattice site to another. Considering two rare earth lattice sites, they are related by the indirect exchange between f electrons through c conduction electrons (RKKY interaction). The magnitude of this coupling J_{cf} was assessed for 1D lattice by Doniach[4] in a magnetic phase diagram involving a competition between the RKKY (Ruderman-Kittel-Kasuya-Yosida) mechanism, which favors the paramagnetic state in the weak-coupling region (small J_{cf}), and the Kondo screening, which leads to the formation of tightly bound singlets in the strong-coupling region (large J_{cf}). Between these two regimes magnetic (Kondo) systems are found with reduced magnetic moments due to the Kondo effect.

Although the Ce ($4f$) band is much narrower than the U ($5f$) band, the Ce ($4f$) electrons may be regarded as itinerant electronic states in as far as ambient pressure conditions are fulfilled. Being the first element in the series, cerium is considered as a border case where the degree of delocalization depends on the applied pressure as well as on the crystal environment. In electronic structure calculations this delicate situation is addressed through various approaches treating the $4f$ states either as atomic like core states or as itinerant in the framework of the local spin density approximation LSDA[5] to the density functional theory DFT.[6] This duality was experimentally evidenced in a combined analysis of μSR (muon spin relaxation) and neutron experiments on cerium intermetallic systems which reveals the existence of magnetic excitations due to both conduction electrons at the Fermi level and well localized f electrons.[7] Regarding the lattice environment, the quantum mixing (hybridization) of the $4f$ states with those of the ligand states can have large effects as well. This involves chemical bonding properties, which are dependent of the crystal lattice properties (structure and interatomic distances).

Generally compounds based on cerium are magnetically ordered at normal pressure and become nonmagnetic at high pressures. Insertion of light elements such as hydrogen can mimic negative pressures with drastic effects on the magnetic properties of Ce based intermetallics. In CeNiIn we identified a transition from an intermediate valence state to a ferromagnetic behavior upon hydrogen insertion.[8] On the contrary CeCoGe which orders antiferromagnetically at $T_N=5.0(2)$ K shows an unexpected magnetic behavior upon hydrogen intake. The observation of a broad peak around 7(1) K in the temperature dependence of the magnetic susceptibility of the hydride CeCoGeH suggests that it presents spin fluctuation behavior.[9] This is somewhat peculiar since the expected schematic trend should lead to a contrary one: The expansion of the lattice by hydrogen intake should lead to an enhancement of the localization of the $4f$ states due to less quantum mixing between them on one hand and with the valence states of the ligands on the other hand, whence the increase of the local magnetic moment as we formerly observed in hydrides of CeNiIn[10] and YFe_2.[11] From this the purpose of the present investigation is to provide a quantum approach within the DFT to the description of the electronic and magnetic structures as well as the bonding characteristics within ternary silicide CeCoSi, isostructural to CeCoGe, and its hydride system. Previous investigation devoted to the magnetic properties of CeCoSi indicates that (i) the cerium is in a trivalent state and (ii) no magnetic transition is observed above 1.6 K.[12]

In this paper, we present a reinvestigation of the electrical and magnetic properties of the silicide CeCoSi and demon-

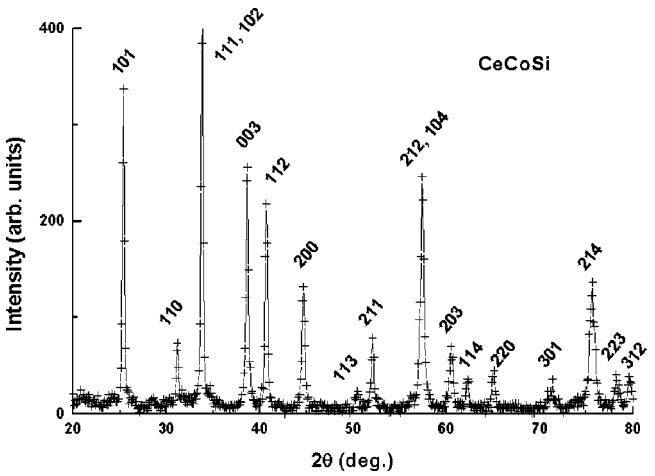

FIG. 1. X-ray diffraction pattern of CeCoSi.

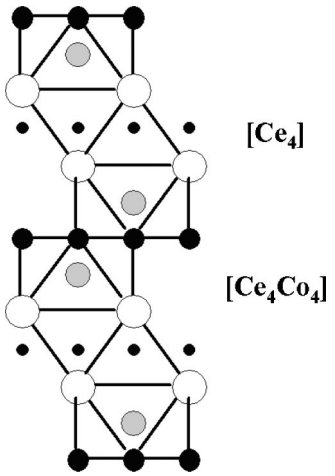

FIG. 2. Projection onto the (a), (c) plane of the crystal structure of CeCoSiH (Ce, Co, Si, and H atoms are, respectively, represented by white large, black medium, grey medium, and black small circles).

strate the existence of an antiferromagnetic transition at $T_N = 8.8(2)$ K. It is shown that this ternary silicide forms the stable hydride CeCoSiH when it is exposed to hydrogen at 523 K under a pressure of $P(H_2) = 4$ MPa. The investigation of magnetic properties of the latter hydride, isostructural to CeCoGeH, reveals a spin fluctuation behavior below $T_{sf} = 130(5)$ K. These results are discussed on the basis of the electronic structures of CeCoSi and CeCoSiH using band structure calculations for the description of the electronic and magnetic structures as well as the bonding characteristics. Also, a similar, calculation for $CeCo_2Si_2$ is presented for comparison; this valence fluctuating system exhibits many structural characteristics with CeCoSi and its hydride.[13]

II. EXPERIMENTAL DETAILS

A. Synthesis and hydrogen absorption

A polycrystalline CeCoSi sample was synthesized by arc melting a stoichiometric mixture of pure elements (purity above 99.9%) in a high-purity argon atmosphere. Then, the sample was turned and remelted several times to ensure homogeneity. Annealing was done for one month at 1073 K by enclosing the sample in an evacuated quartz tube. Its x-ray powder pattern is fully indexed on the basis of a tetragonal unit cell with the CeFeSi-type structure (Fig. 1). No parasitic phase is detected. The unit cell parameters deduced from this investigation $a = 0.4041(2)$ nm and $c = 0.6990(2)$ nm agree with those reported previously.[12]

Hydrogen absorption experiments were performed using the apparatus formerly described.[14] An annealed ingot was heated under vacuum at 523 K for 12 h and then exposed to 4 MPa of hydrogen gas at the same temperature. The amount of H absorbed was determined volumetrically by monitoring pressure changes in a calibrated volume. Under the experimental conditions described above, CeCoSi absorbs hydrogen. The amount of H-atom inserted is 1.0(1) per CeCoSi formula. The hydride formed is stable in air and shows a metallic aspect. Also, the H-absorption induces a decrepitating in small grains of the pure starting ingot.

X-ray powder diffraction with the use of a Philips 1050-diffractometer (Cu $K\alpha$ radiation) was applied for the characterization of the structural type and for the phase identification of the samples. The unit cell parameters were determined by a least-squares refinement method using silicon (5 N) as an internal standard.

Magnetization measurements were performed using a Superconducting Quantum Interference Device (SQUID) magnetometer in the temperature range 1.8–300 K and applied fields up to 5 T. Electrical resistivity was measured above 4.2 K on a polycrystalline sample using standard dc four-probe measurements.

B. Structural, electrical, and magnetic properties

The investigation of the structural properties of the hydride $CeCoSiH_{1.0(1)}$ using x-ray powder diffraction indicates that it crystallizes in the tetragonal CeCoGeH-type structure[9] (space group $P4/nmm$) with $a = 0.3955(2)$ nm and $c = 0.7861(3)$ nm as unit cell parameters. This structure can be described by a stacking along the c axis of two layers formed by $[Ce_4Co_4]$ antiprisms and separated by one layer of $[Ce_4]$ pseudotetrahedral units (Fig. 2). The $[Ce_4Co_4]$ antiprisms surrounding the Si atom are also observed in the crystal structure of the ternary silicide $CeCo_2Si_2$.[13] The H atoms are inserted in the $[Ce_4]$ pseudotetrahedral sites (2b)-site $(\frac{1}{4}, \frac{3}{4}, \frac{1}{2})$ giving interatomic distances $d_{Ce-H} = 0.2391(2)$ nm between Ce and H atoms.

The crystal structure of CeCoSi and its hydride adopt the same space group but the hydrogenation of this ternary silicide causes a pronounced anisotropic expansion of the unit cell; the a-parameter decreases from 0.4041(2) nm to 0.3955(2) nm (−2.1%) whereas the c parameter increases strongly from 0.6990(2) nm to 0.7861(3) nm (+12.5%). In other words, the insertion of hydrogen into CeCoSi involves an expansion of the unit cell volume from 0.1141(2) nm^3 to 0.1230(4) nm^3 (+7.8%). These structural characteristics are comparable to those reported recently during the hydrogenation of the ternary germanide CeCoGe.[9]

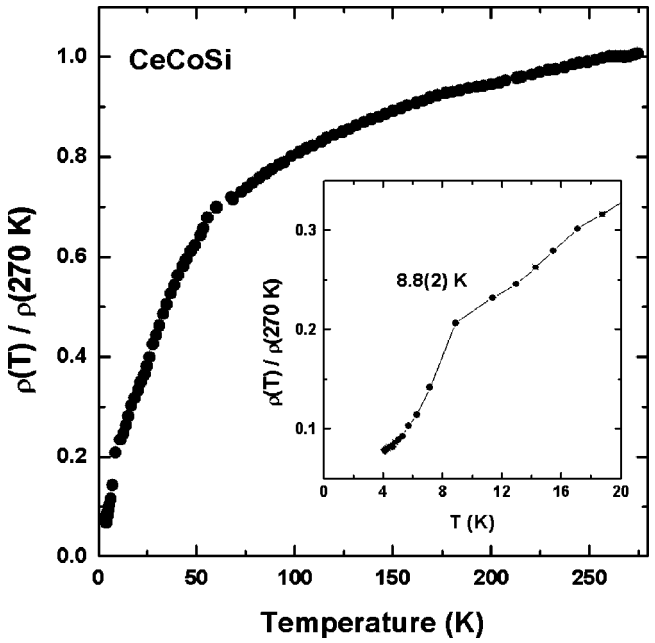

FIG. 3. Temperature dependence of the reduced electrical resistivity for ternary silicide CeCoSi (inset for $T \leqslant 20$ K).

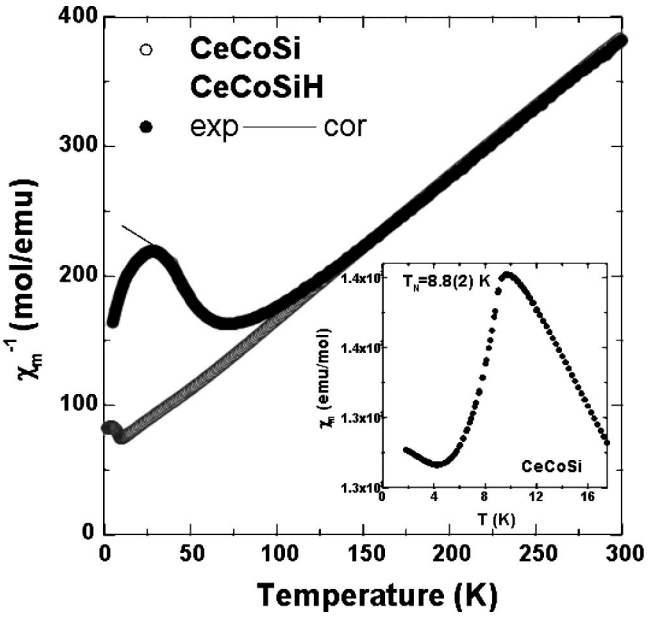

FIG. 4. Temperature dependence of the reciprocal magnetic susceptibility χ_m^{-1} measured with an applied field $\mu_0 H = 4$ T of silicide CeCoSi and its hydride. Solid line shows for the hydride, the corrected data $(\chi_m - nC/T)^{-1}$. Inset: $\chi_m = f(T)$ at low temperature for CeCoSi.

The hydrogenation of CeCoSi induces important changes in the values of the $d_{\text{Ce–Ce}}$ distances; those located in the (a,b)-plane decrease (0.4041–0.3955 nm) whereas the four other increase (0.3725–0.3878 nm). The pseudotetrahedral $[Ce_4]$ unit is less distorted in the hydride CeCoSiH. It is also worth pointing out that the $d_{\text{Ce–Ce}}$ distances (0.3955 nm) existing in the (a,b)-plane for hydride CeCoSiH are comparable to those observed (0.3958 nm) in the ternary silicide $CeCo_2Si_2$.[13] We shall be using these experimental crystal data for the calculations of the electronic and magnetic structures of the different systems.

Figure 3 displays, above 4.2 K, the temperature dependence of the reduced electrical resistivity of CeCoSi. (*Due to the presence of microcracks in the polycrystalline sample, absolute value of ρ could not be determined accurately; for this reason, a reduced representation is chosen.*) In the temperature range from 270 to 100 K, the resistivity ρ shows a slight decrease with decreasing temperature. Then, the curve $\rho(T)/\rho(270\ \text{K}) = f(T)$ exhibits two characteristics: (i) a curvature around 60–70 K and (ii) a sharp decrease at 8.8(2) K (inset of Fig. 3). The former is likely to be associated with the interplay between Kondo and crystalline electric field (CEF) effects as found for many intermetallics based on cerium such as CeRhGe and CePtGe.[15] The latter suggests the occurrence of a magnetic ordering below 8.8(2) K. The decrease of ρ below this temperature could be associated to the loss of spin disorder scattering of the conduction electrons owing to the appearance of a magnetic transition.

In order to investigate this possible magnetic ordering, we have performed magnetization measurements on CeCoSi. Above 70 K, its reciprocal magnetic susceptibility follows a Curie–Weiss law with the effective magnetic moment $\mu_{\text{eff}} = 2.71(5)\ \mu_B/\text{mol}$ and the paramagnetic Curie temperature $\theta_p = -55(1)$ K (Fig. 4). These values are close to those reported previously by Welter *et al.*,[12] respectively 2.8 μ_B/mol and −53 K. The presence of a sharp peak at $T_N = 8.8(2)$ K in the temperature dependence of the magnetic susceptibility of CeCoSi (inset of Fig. 4), suggests an antiferromagnetic ordering of the Ce moments. This behavior agrees with the electrical properties of CeCoSi at low temperatures. It should be mentioned here that Welter *et al.*[12] found no magnetic transition above 4.2 K in CeCoSi while we have been able to detect a magnetic transition using a smaller applied magnetic field of 0.05 T (1 T in Ref. 12) for the magnetization measurements. Since our sample is of high quality as revealed by x-ray powder diffraction, microprobe analysis and the large value of the residual resistivity ratio **(**$\rho(270\ \text{K})/\rho(4.2\ \text{K}) \cong 25$**)**, we believe the magnetic transition is intrinsic. Other experiments such as neutron powder diffraction and specific heat measurements are planned in order to confirm this magnetic transition.

The curve $\chi_m^{-1} = f(T)$ relative to CeCoSiH shows a different behavior (Fig. 4): (i) above 150 K, χ_m^{-1} follows a Curie–Weiss law with the parameters $\mu_{\text{eff}} = 2.72(5)\ \mu_B/\text{mol}$ and $\theta_p = -56(1)$ K (ii) the presence of a broad minimum around 70 K is a characteristic of valence fluctuating systems as reported earlier;[16] (iii) the decrease of χ_m^{-1} below 25 K might originate from a small amount of free Ce^{3+} ions stabilized on lattice defects or a trace of some paramagnetic impurities, as often observed in other valence fluctuating systems.[17] According to this scheme, the magnetic susceptibility χ_m of the hydride CeCoSiH can be expressed at low temperatures ($T < 25$ K) by $\chi_m = \chi_m(0) + nC/T$ where $\chi_m(0)$ is the magnetic susceptibility at $T = 0$ K, n is the proportion of stable Ce^{3+} moments composing the trace of magnetic impurities and $C = 0.807$ emu K/mol is the Curie constant for free Ce^{3+}

ions. The best agreement between experimental and calculated χ_m values leads to $\chi_m(0)=3.85(8)\times10^{-3}$ emu/mol and $n=13.6(6)\times10^{-3}Ce^{3+}$ ions/mol. Figure 4 presents the corrected $[\chi_m - nC/T]^{-1}=f(T)$ reciprocal magnetic susceptibility versus temperature resulting from this calculation. This curve goes through a large minimum near 65(3) K. With the model offered by Lawrence *et al.*[16] we estimate $T_{sf}=130(5)$ K as the spin fluctuation temperature resulting from the hybridization between $4f$(Ce) and conduction electrons. This analysis suggests that the hydrogenation of CeCoSi leads to the transition antiferromagnet → spin fluctuation behavior.

III. THEORETICAL FRAMEWORK AND COMPUTATIONAL RESULTS

Computations are all *ab initio* and self consistent (crystal data and neutral atoms as input) within the local spin density approximation to the density functional theory. More specifically, we use the scalar relativistic implementation of the augmented spherical wave (ASW) method based on the atomic sphere (ASA) approximation.[18,19] All valence electrons, including $4f$ (Ce) were treated as band states. In the minimal ASW basis set, we chose the outermost shells to represent the valence states and the matrix elements were constructed using partial waves up to $l_{\max}+1=4$ for Ce, $l_{\max}+1=3$ for Co and $l_{\max}+1=2$ for Si. In a first step the calculations were carried out assuming nonmagnetic configurations (non-spin-polarized NSP), meaning that spin degeneracy was enforced for all species. Such a configuration is however not relevant to a paramagnet which would only be simulated by a huge supercell entering random spin orientations over the different magnetic sites. Then within spin polarized calculations spin only moments were accounted for leading to an implicit long range ferromagnetic order. Further in order to provide a model for the experimentally observed antiferromagnetic ground state we have envisaged a doubling of the unit cell along the *c* axis. In view of nonavailable neutron diffraction characterizations this provides one possible model of a long range AF spin structure which should be validated as a ground state configuration from the relative energies of band theoretical calculations. Orbital effects can be large in uranium based systems and to a lesser extent within cerium intermetallic systems. We discussed these issues in a comparative review for A_2T_2Sn ($A=U$, Ce; $t=$Ni, Pd) systems[3] in which the effects of spin-orbit coupling and orbital polarization were investigated using different schemes.[1] Last, in order to represent the correct shape of the crystal potential in the hydrogen free CeCoSiH which we study to assess magnetovolume effects, additional augmentation spheres called empty spheres (ES, zero atomic number) were inserted at H positions.

The results obtained from DFT based calculations provide accurate indications to quantities regarding the magnitudes of the magnetic moments, the nature and energy position of the states with respect to the Fermi level, the ground state configuration from relative energies, however one needs a more elaborate tool of information about the nature of the interaction between atomic constituents. Such information can be provided in the framework of the overlap population (OP) which involves the overlap matrix leading to the so-called crystal orbital overlap population (COOP)[20] or alternatively introducing the Hamiltonian based population crystal orbital Hamiltonian population (COHP).[21] Both approaches provide a qualitative description of the chemical interactions between two atomic species by assigning a bonding, nonbonding or antibonding character. A slight refinement of the COHP was recently proposed in form of the "covalent bond energy" E_{COV} which combines both COHP and COOP so as to make the resulting quantity independent of the choice of the zero of potential.[22] The E_{COV} parametrization was recently implemented within the ASW method.[23] Our experience with both COOP and E_{COV} shows that they give similar general trends although COOP exagerate the magnitude of antibonding states. We shall be using the E_{COV} description of the chemical bond in this work.

A. Calculations and results of the non-spin-polarized configurations

Beside CeCoSi and CeCoSiH additional calculations were done for $CeCo_2Si_2$ which shows similar structural characteristics with the CeCoSi system and its hydride. Furthermore, the CeCoSi system was examined at the hydride lattice constant. In the framework of the ASW method this is made possible by replacing the hydrogen atoms by "empty spheres," i.e., pseudo atoms with zero atomic number. The purpose is to evidence the magnetovolume effect of hydrogen versus its chemical effect.[10]

1. Density of states DOS

The site projected DOS for the four systems are given in Figs. 5 and 6. In all panels the Fermi level (E_F) is taken as zero energy. The cerium DOS are seen to prevail through the large peak around E_F mainly due to ($4f$) Ce states which show larger localization (sharper and narrower peaks vs Fig. 5) in the hydride system [with H Fig. 5(b) or without H Fig. 6(b)]. This is concomitant with a larger cell volume whereby the average Ce–Ce separation is higher. But there is a non-negligible contribution from Ce itinerant states below E_F which ensure for the chemical bonding through the hybridization with Co and Si states as well as with hydrogen as it will be shown below. Due to the large filling of their *d* states, cobalt DOS are found completely within the valence band. They show similar shape at the low energy part of the VB, i.e.,
$[-6,-2\ \text{eV}]$ which is a feature pointing to a mixing between Co, Si, and Ce. Within the hydride system [Fig. 5(b)] hydrogen DOS were artificially multiplied by 5 in order to clearly exhibit their contribution within the VB. They can be seen to have a similar skyline to other states between −5 and −4 eV, however a significant intensity just above −4 eV points to a mixing with Ce itinerant states (see chemical bonding section). The absence of H DOS in the hydrogen free CeCoSi [Fig. 6(b)] and the larger magnitude of ($4f$) Ce DOS at the Fermi level $n(E_F)$, are features which differentiate it from the hydride DOS. The lower energy lying regions of the ($4f$) Ce DOS are crossed by E_F, with a larger magnitude for CeCoSi as well as the "hydrogen free CeCoSiH" than for the hydride

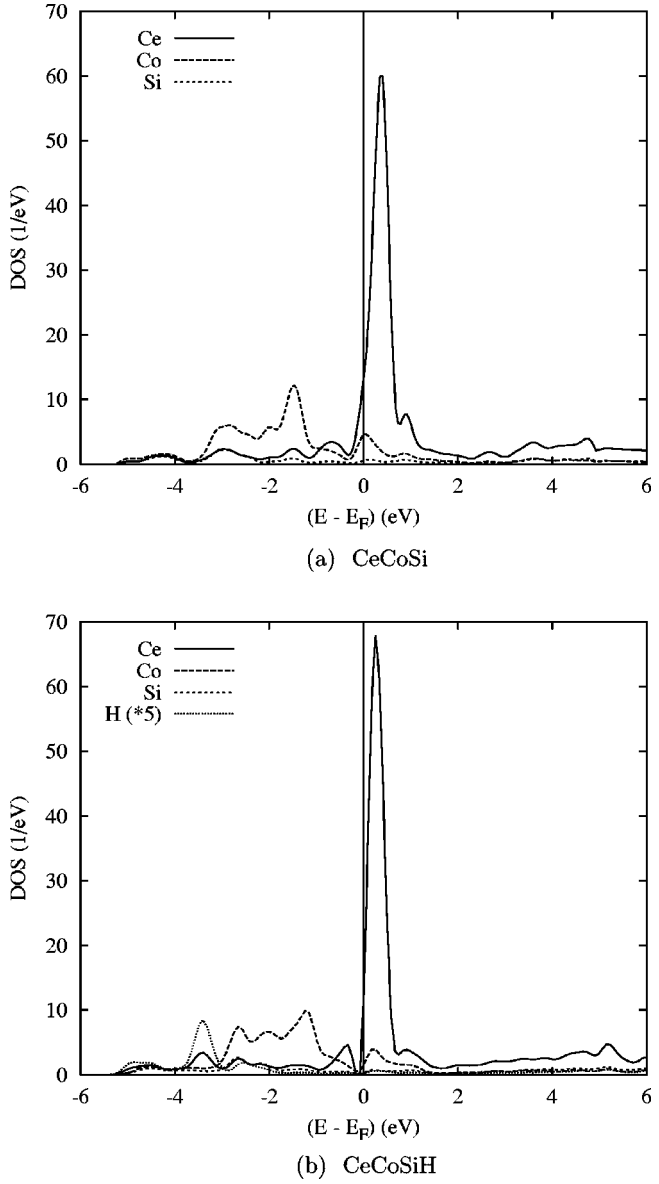

FIG. 5. Nonmagnetic site projected DOS of (a) CeCoSi and (b) CeCoSiH.

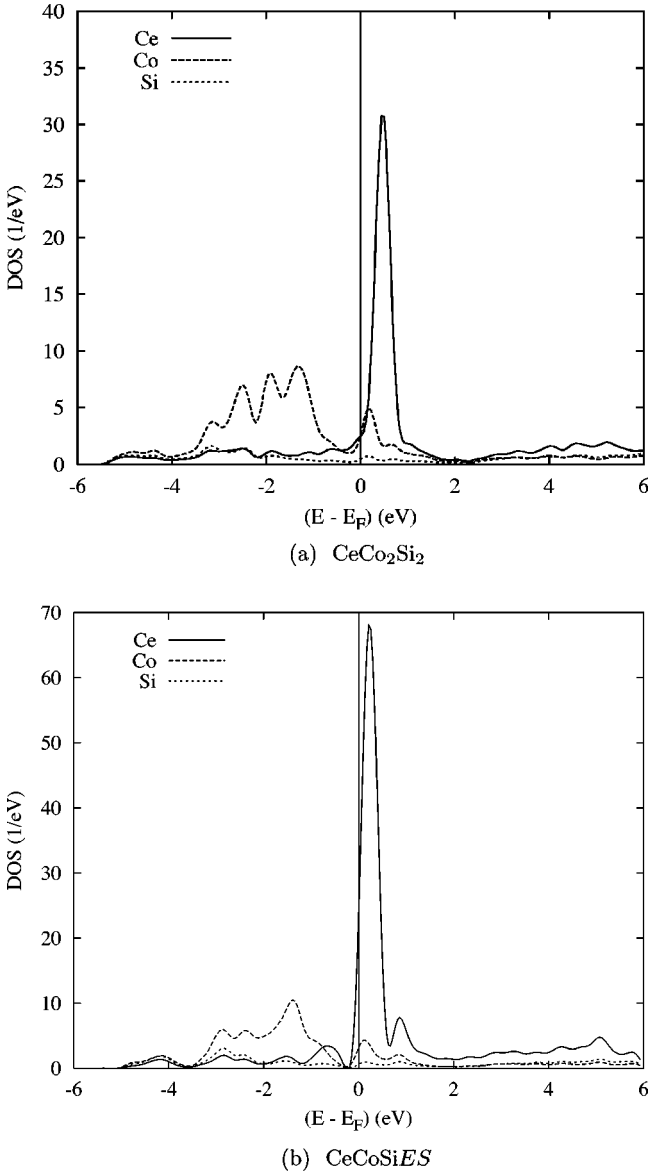

FIG. 6. Nonmagnetic site projected DOS of (a) $CeCo_2Si_2$ and (b) CeCoSi*ES*.

and $CeCo_2Si_2$ Fig. 6(a); this will have consequences on the magnetic properties of the relevant systems as it will be analyzed in the next paragraph. Silicium states contribute to the bonding essentially with cobalt such as in $CeCo_2Si_2$ silicide and do not show significant differences between the studied compounds. A more reliable determination of the two body interactions can be obtained from chemical bonding criteria within the covalent bond energy E_{COV} framework described above. This is carried out in subsequent sections of this work.

2. Analysis of the NSP-DOS within Stoner theory

In as far as $(4f)$ Ce and $(3d)$ Co states were treated as band states in the framework of our calculations the Stoner theory of band ferromagnetism[24] can be applied to address the spin polarization. Formulating the problem at zero temperature (ground state) one can express the total energy of the spin system resulting from the exchange and kinetic energies counted from a non-magnetic state as follows:

$$E = \frac{1}{2}\left[\frac{m^2}{n(E_F)}\right][1 - \mathbf{I}n(E_F)].$$

Here $\mathbf{I}$ is the Stoner exchange-correlation integral which is an atomic quantity that can be derived from spin-polarized calculations (nonrelativistic, scalar, and fully relativistic)[25] and $n(E_F)$ is the DOS at E_F in the nonmagnetic state. From this expression the product $\mathbf{I}.n(E_F)$ provides a criterion for the stability of the spin system. A nonmagnetic configuration (equal occupation of the two spin states) towards spin-polarization (unequal spin occupation) will be unfavorable if $\mathbf{I}.n(E_F) > 1$. The system then stabilizes through a gain of energy due to exchange.

Among the four studied systems, cerium shows a large $n(E_F)$ for CeCoSi and for the hydrogen free hydride system, while there is a minimum for the hydride and $CeCo_2Si_2$. To analyze these results we use the Stoner integral for Ce from former scalar relativistic calculations[3] $\mathbf{I}(\mathrm{Ce}\ 4f) \sim 0.26$ eV and $\mathbf{I}(\mathrm{Co}\ 3d) \sim 0.49$ from the original work of Janak.[25] For Co the Stoner product is obtained larger than 1 only within CeCoSi. For Ce, the corresponding Stoner products $\mathbf{I}.n(E_F)$ for $4f$ are, respectively, 1.7, 0.20, 0.54, and 2.19 within CeCoSi, CeCoSiH, $CeCo_2Si_2$, and the hydrogen-free CeCoSiH. The Stoner criterion is obeyed only for those magnitudes larger than one; this leads to propose that Ce as well as Co should carry a magnetic moment in CeCoSi while only Ce should polarize within the expanded cell of CeCoSi at the hydride volume. These qualitative conclusions agree with the experimental observations of a magnetically ordered state only within the CeCoSi system among the studied series. The unexepected result for the expanded CeCoSi lattice as with respect to the actual hydride introduces significant implications involving that the chemical bonding of H with its surrounding atoms annihilates the magnetovolume effect brought by the lattice expansion which should have enhanced the onset of an ordered moment on Ce.

3. Covalent bond energy: E_{COV}

From the results of NSP calculations the chemical bonding can be addressed. This is related to the fact that the spin polarized bands, to a large degree, result from the NSP bands by a rigid energy shift. Hence it is well justified to discuss the chemical bonding already from the NSP results. Because of their little involvement with the bonding $(4f)$ Ce orbitals were discarded from the analysis. Negative, positive, and zero covalent bond energies along the y axis are relative to bonding, antibonding and nonbonding states, respectively. In Figs. 7(a) and 7(b) we make explicit the E_{COV} for Ce−Co, Ce−Si, and Co−Si pair interactions which determine the nature of the bonding within the pristine and hydrided ternary systems. The plots for $CeCo_2Si_2$ and the hydrogen free expanded system show similar features and they will not be shown here. Co−Si interaction is observed to be prevailing with respect to Ce−Co then to Ce−Si which is weakest. The major part of the VB is bonding with antibonding interactions starting to appear in the neighborhood of E_F especially for Co−Si. The difference appears as well for the Ce−Co interaction which shows a larger overall magnitude in CeCoSi than in CeCoSiH for which antibonding Ce−Co interactions are observed at ~ -2 eV. The minimum E_{COV} at E_F in Fig. 7(b) is concomitant with a minimum DOS in Fig. 5(b). The small differences between the E_{COV} in Figs. 7(a) and 7(b) show that both systems are similar from the chemical point of view so that the relevant differences brought by the insertion of hydrogen can be discussed based on its interaction with the three species from the CeCoSi lattice is built.

Figure 7(c) gives the metal-hydrogen contribution to the bonding. Here the prevailing bonding is for the Ce−H interaction which is bonding throughout the whole energy range, from −4 eV up into the CB. On the contrary there is a strong antibonding contribution for Co−H around −2 eV. Both Ce−H and Co−H interactions show similar shapes around

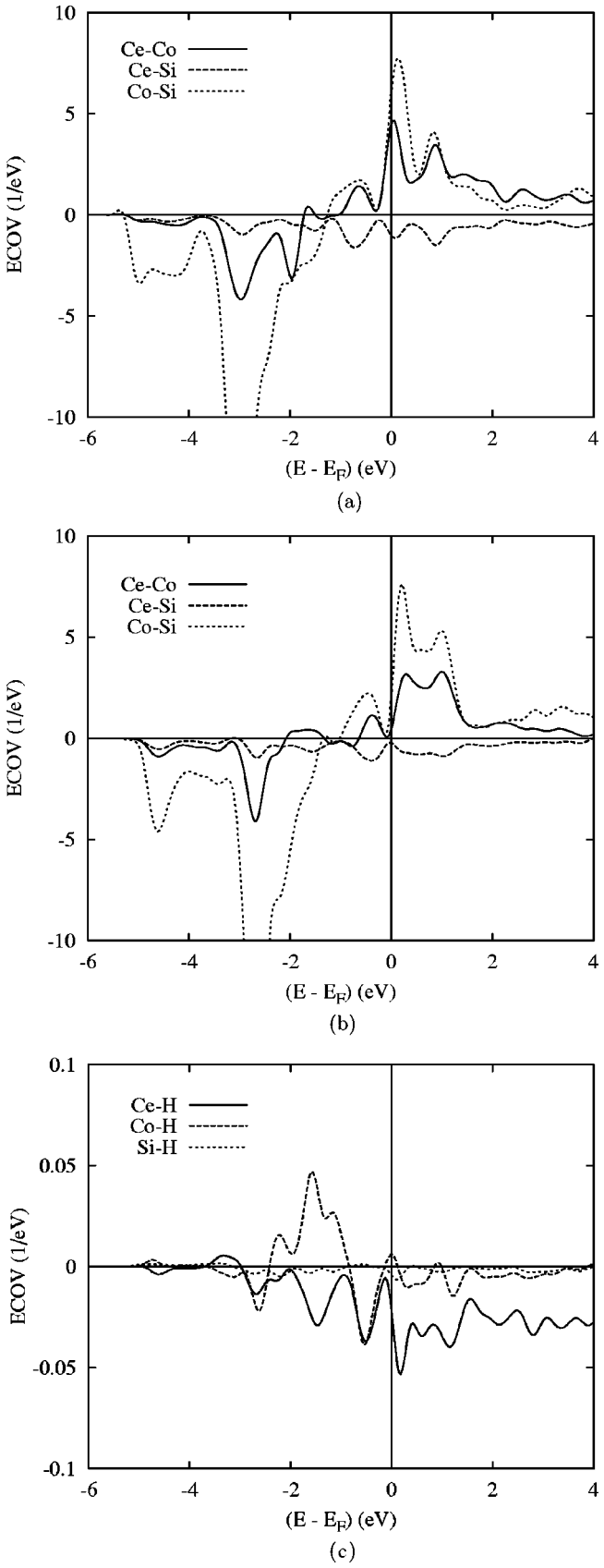

FIG. 7. E_{COV} for Ce−Co, Ce−Si interactions in (a) CeCoSi and (b) CeCoSiH and Ce−H, Co−H, and Si−H interactions in (c) CeCoSiH.

−3 and −1 eV on both sides of the antibonding region. Albeit small in their magnitudes such E_{COV} changes brought by hydrogen should be at the origin of the different behaviors of CeCoSi and CeCoSiH, i.e., in their prevailence over the volume effect.

B. Results of the spin polarized configurations

1. Energies and magnitudes of the spin only moments

Spin-polarized calculations for the magnetic structures were carried out by initially allowing for two spin occupations and then self-consistently carry out convergence for the charges and the magnetic moments. We assume a ferromagnetic *F* configuration with no constraint on spins then antiferromagnetic *AF* computations are carried out for the experimentally evidenced *AF* ground state of CeCoSi. The results confirm the trends of the Stoner mean field analysis of the NSP results by the onset of magnetization only within the nonhydrided material as well as within the expanded CeCoSi system with a stabilization of the spin polarized configuration by $\Delta E \sim 0.04$ eV per unit cell. The spin-only moments are $M(\mathrm{Ce}) = 0.84\ \mu_B$, $M(\mathrm{Co}) = -0.25\ \mu_B$ with a total magnetization of 1.18 μ_B per unit cell (2 fu). For the expanded CeCoSi simulating the volume effect of hydrogen, the results are $M(\mathrm{Ce}) = 0.93\ \mu_B$, $M(\mathrm{Co}) = -0.009\ \mu_B$ with a total magnetization of 1.84 μ_B per unit cell (2 fu). The antiparallel spin alignment between Ce and Co is an indication of an induced moment on the latter due to the quantum mixing of its states with those of Ce within the VB. The change of magnitude between the calculated moments is due to the increase of $d_{\mathrm{Ce–Co}}$ from 0.306 to 0.325 nm. From these results the major effect is in the enhancement of the spin moment on Ce due to the lattice expansion. This gives hydrogen a major chemical effect in changing the magnetically ordered CeCoSi into a spin fluctuation behavior system. These results are opposed to those of spin fluctuation hexagonal CeNiIn system for which the hydride $\mathrm{CeNiInH}_{1.8}$ is found magnetically ordered.[8,10]

In order to provide a model for the experimentally observed antiferromagnetic ground state we envisaged one solution of doubling the unit cell along the *c* axis. In view of the nonexistence of precise neutron diffraction characterizations, (these works are underway), this provides one possible model of a long range AF spin structure. The total energy results show a slight energy difference of $\Delta E \sim 0.02$ eV per CeCoSi cell in favor of the AF configuration. Although Co moment keeps an antiparallel alignment with respect to Ce moment, the magnitude of the latter strongly decreases down to 0.41 μ_B. We note here that we use the energy differences from calculations carried out in similar conditions (ex. of Brillouin zone **k**-points sampling) to evaluate relative stabilities. These energies are not related to temperatures; note that 1 eV = 11 604.45 K would lead to absolute values: $\Delta E_{\mathrm{NSPCo–HFerro}} \sim 0.04$ eV ≡ 464 K and $\Delta E_{\mathrm{FerroCo–HAF}} \sim 0.02$ eV ≡ 232 K, which would translate temperature magnitudes beyond any magnetic transitions observed for our systems.

2. Spin orbit coupling effects

It is well known that relativistic effects like spin orbit coupling (SOC) have considerable influence on the formation of magnetic moments in narrow band systems such as those based on 4*f* and 5*f* elements. This is of particular importance in the latter where the size of the SOC splitting is of the order of magnitude of the 5*f* band width. In contrast to 3*d* transition elements the localized character of the *f* wave function also leads to the formation of orbital moments. Various attempts have been made in order to include these narrow band correlations into *ab initio* calculational schemes. The computation of the orbital moment from scalar relativistic scheme built within the LSDA can provide the correct sign of the orbital moment *versus* spin moment in agreement with Hund's rule (opposite sign for less than half filled *nf* subshell and same sign for more than half-filled subshell) but the magnitude of the moment is not sufficient enough to reproduce the experimentally observed ordered moments. Stronger correlations leading to obeying the Hund's second rule for localized electronic states can be accounted for through the orbital field (OR) scheme introduced by Brooks[1] and Sandratskii and Kübler.[26] Using this scheme we correctly computed[3] the spin orbit coupling within $\mathrm{Ce_2Pd_2Sn}$ system leading to a good approach of the experimental results. As a matter of fact, in this intermetallic system as well as in other ones investigated by us, a general trend is that the magnitude of the orbital moment (L) is close to that of the spin-only (S.O.) moment ($\mathrm{Ce_2Pd_2Sn}$: S.O./L = 0.78/−0.93). Their opposite sign agrees with Hund's rule. The orbital moment of cerium stems from a 4*f* (Ce) occupation of about 1.3 electrons (which is equally found in presently studied systems) whose orbital moment (∼2.5 μ_B) comes close to the one of an atomic orbital, namely 3 μ_B as expected from Hund's second rule. This reflects the atomic like character of the 4*f* (Ce) shell. For CeCoSi an ordered LS moment of cerium of ∼1.7 μ_B is found for the ferromagnetic configuration while a larger magnitude (∼2.1 μ_B) arising from the smaller spin only moment within the AF configuration is obtained. The computed values should be confronted with experimental magnetizations from neutron diffraction when they are made available.

3. Density of states of the magnetic configurations

The effects of spin polarization for the CeCoSi and for the expanded lattice are illustrated for the site and spin projected DOS given in Fig. 8; in as far as these are negligible for CeCoSiH and $\mathrm{CeCo_2Si_2}$ their SP DOS are not shown here. The site projected DOS show an energy shift between the electron populations for the majority (↑) and minority (↓) spin populations mainly for Ce which carries a magnetic moment. The induced nature of cobalt moment can be seen through the slight negative shift as opposed to the Ce partial DOS between the up- and downspin populations Fig.8(a). This is no longer observed for the expanded lattice Co-DOS 8(b) for which the spin moment on cobalt is very small as discussed above. There is a stronger localization of (4*f*) Ce states in the expanded CeCoSi lattice [Fig. 8(b)] due to a larger separation between the Ce sites which is concomitant with the larger moment of Ce.

For sake of completeness Fig. 9 gives the total DOS for the AF ground state configuration. They can be seen to have

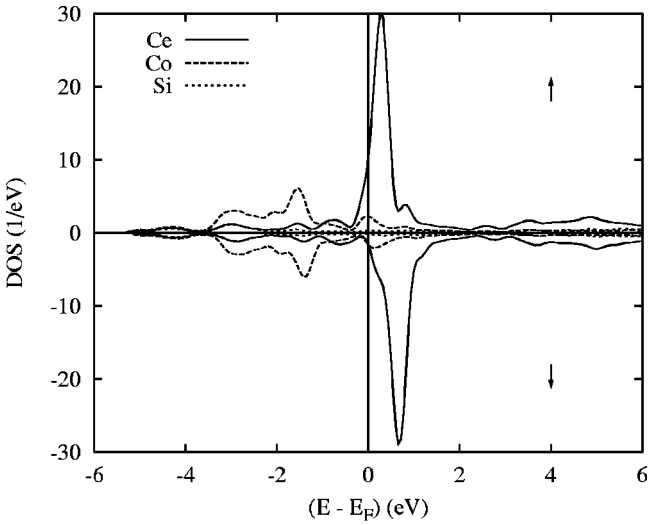

(a) CeCoSi

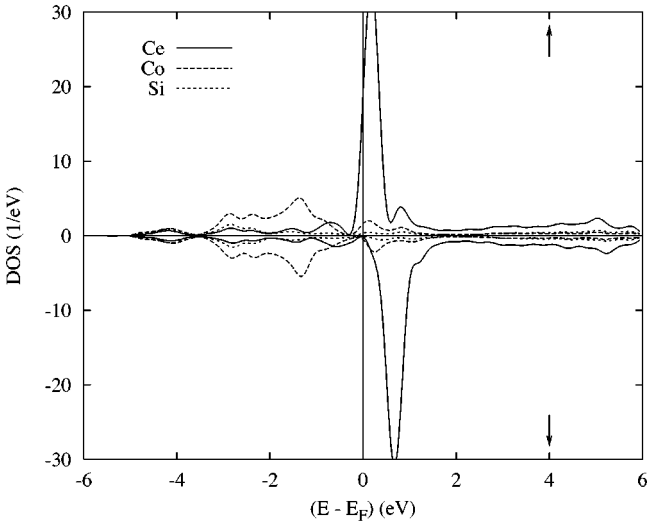

(b) CeCoSiES_H

FIG. 8. Spin polarized site projected DOS of CeCoSi at (a) experimental and (b) expanded lattice of hydride.

similar weights ↑ and ↓ for all species. This is exemplified for partial Ce DOS plotted under the total DOS curve.

IV. CONCLUSION AND OUTLOOK

In this work we have undertaken experimental and theoretical investigations of the hydrogen insertion effects on the magnetic behavior of CeCoSi equatomic system. Contrary to formerly studied cerium equiatomic systems such as CeNiIn

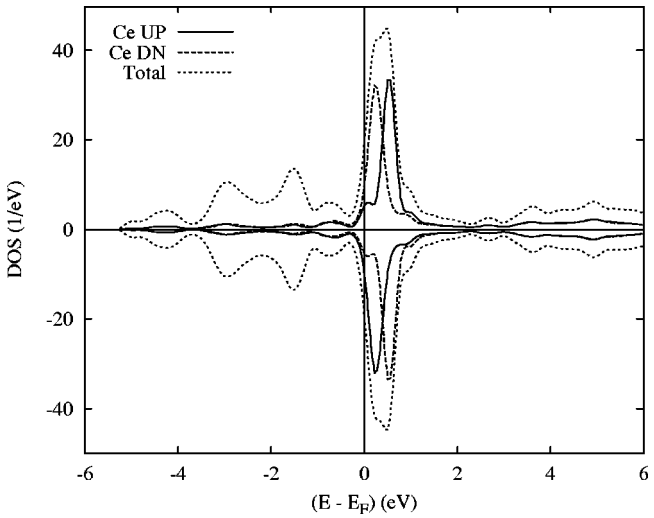

FIG. 9. Antiferromagnetic DOS for Ce ↑ and ↓ spin and total DOS of CeCoSi in the ground state.

the antiferromagnetic behavior of CeCoSi changes to spin fluctuation upon hydrogen absorption. In order to further address this peculiar feature we have undertaken *ab initio* computations within the local spin density functional theory for CeCoSi, for the hydride CeCoSiH as well as for the expanded CeCoSi system at the hydride volume. The analysis of the electronic structures and of the chemical bonding properties using the covalent bond energy lead to suggest that the chemical effect of hydrogen prevails over cell expansion which would enhance the magnetization otherwise. A possible antiferromagnetic structure with a propagation along the c axis was proposed for CeCoSi ground state which is experimentally evidenced in this work from magnetic measurements.

Further ongoing experimental and theoretical works reporting on cerium hydride systems prepared and investigated in our Institute, such as the series: Ce$TX'H'$ (T=3d, 4d, 5d transition metal and X=p-metal isochemical to In, such as Al) should allow to draw out systematics on the magnetic behavior of the cerium equiatomic systems.

ACKNOWLEDGMENTS

Computational facilities were provided within the Intensive Numerical Simulation Facilities Network M3PEC of the University Bordeaux 1 partly financed by the "Conseil Régional d'Aquitaine." Critical reading of the manuscript by Dr. Volker Eyert (University of Augsburg, Germany) is gratefully acknowledged.

*Corresponding author. Email address: matar@icmcb-bordeaux.cnrs.fr

[1] M. S. S. Brooks and B. Johansson, in *Handbook of Magnetic Materials*, edited by K. H. J. Buschow (North-Holland, Amsterdam, 1993), Vol. 7.

[2] G. R. Stewart, Rev. Mod. Phys. **73**, 797 (2001).

[3] S. F. Matar and A. Mavromaras, J. Solid State Chem. **149**, 449 (2000).

[4] S. Doniach, Physica B **91**, 231 (1977).
[5] J. von Barth and D. Hedin, J. Phys. C **5**, 1629 (1972); J. F. Janak, Solid State Commun. **25**, 53 (1978).
[6] W. Kohn and L. J. Sham, Phys. Rev. A **140**, 1133 (1965); P. Hohenberg and W. Kohn, Phys. Rev. B **136**, 864 (1964).
[7] P. Dalmas de Réotier, A. Yaouanc, P. C. M. Gubbens, C. T. Kaiser, A. M. Mulders, S. P. Cottrell, and P. J. C. King, ISIS Rep. (1998).
[8] B. Chevalier, M. L. Kahn, J.-L. Bobet, M. Pasrurel, and J. Etourneau, J. Phys.: Condens. Matter **14**, L365 (2002).
[9] B. Chevalier, E. Gaudin, F. Weill, and J.-L. Bobet, Intermetallics **12**, 437 (2004).
[10] S. F. Matar, B. Chevalier, V. Eyert, and J. Etourneau, Solid State Sci. **5**, 1385 (2003).
[11] S. F. Matar and V. Paul-Boncour, C.R. Acad. Sci., Ser. IIc: Chim **3**, 27 (2000); V. Paul-Boncour and S. F. Matar, Phys. Rev. B (to be published).
[12] R. Welter, G. Venturini, E. Ressouche, and B. Malaman, J. Alloys Compd. **210**, 279 (1994).
[13] B. Chevalier, J. Etourneau, J. Rossat-Mignod, R. Calemczuk, and E. Bonjour, J. Phys.: Condens. Matter **3**, 1847 (1991).
[14] J.-L. Bobet, S. Pechev, B. Chevalier, and B. Darriet, J. Alloys Compd. **267**, 136 (1998).
[15] P. Rogl, B. Chevalier, M. J. Besnus, and J. Etourneau, J. Magn. Magn. Mater. **80**, 305 (1989).
[16] J. M. Lawrence, P. S. Riseborough, and R. D. Parks, Rep. Prog. Phys. **44**, 1 (1981).
[17] E. D. Mun, Y. S. Kwon, and M. H. Jung, Phys. Rev. B **67**, 033103 (2003).
[18] A. R. Williams, J. Kübler, and C. D. Gelatt, Jr., Phys. Rev. B **19**, 6094 (1979); V. Eyert, Int. J. Quantum Chem. **77**, 1007 (2000) (for a recent review).
[19] D. D. Kölling and B. N. Harmon, J. Phys. C **10**, 3107 (1977).
[20] R. Hoffmann, Angew. Chem., Int. Ed. Engl. **26**, 846 (1987).
[21] R. Dronskowski and P. E. Blöchl, J. Phys. Chem. **97**, 8617 (1993).
[22] G. Bester and M. Fähnle, J. Phys.: Condens. Matter **13**, 11541 (2001); **13**, 11551 (2001).
[23] V. Eyert (unpublished).
[24] J. Kübler and V. Eyert, in *Materials Science and Technology. Vol. 3A: Electronic and Magnetic Properties of Metals and Ceramics*, Part I. Volume editor K. H. J. Buschow (VCH, Weinheim, 1992), pp. 1–145.
[25] J. F. Janak, Phys. Rev. B **16**, 255 (1977).
[26] L. M. Sandratskii and J. Kübler, Phys. Rev. Lett. **75**, 946 (1995).